NUMERICAL MODELLING OF CONTINUOUS-BIOWASTE COMPOSTING UNDER UPWARD FORCED AERATION IN A CLOSED SYSTEM

Md. Al Amin*[1], Quazi Hamidul Bari[2]

[1] *Postgraduate Student, Khulna University of Engineering and Technology, Bangladesh, e-mail: mdalamin2308@gmail.com*
[2] *Professor, Khulna University of Engineering and Technology, Bangladesh, e-mail: qhbari@ce.kuet.ac.bd*

***Corresponding Author**

ABSTRACT

Biowaste composting relies on microbial degradation under controlled aeration, temperature, and moisture conditions to transform organic waste into usable compost, whereas municipal solid waste is often improperly managed in developing countries This study focuses on biowaste composting in a continuous-flow reactor operated with upward forced aeration in a closed system, using a mathematical model to simulate the spatio-temporal behavior of temperature, moisture, and biodegradable volatile solids across multiple slots and layers. For conducting this study, the reactors consist of seven sequential slots, each containing six vertical layers, through which a waste sample passes to the next slot every three days, to achieve a total composting time of 21 days. A systematic aeration strategy (Air Flow: Qi → Qi/2 → Qi) was incorporated to simulate realistic operational conditions for thermophilic. The Simulation results reveal that the maximum temperature is reached in the Upper Layer (UL) due to concentrated oxygen (around 65 °C), and the Lower Layer (LL) contains a temperature of around 32-38 °C, which is conducive to less microbial growth. Volatile solids reduction of each bio-waste sample was around LL:30-UL:58%, whereas moisture content progressively reduced to 45-48% by Day 21. Oxygen consumption patterns also mirrored biological activity, with minimum concentrations (~16-17%) occurring during the thermophilic peak in Slot 4 out of 7 slots. And the total waste decomposed in the middle layer (L3) was around 52% of the total bio-waste. The model performed well, with relatively high R^2 values (0.61–0.77) between simulated and actual temperatures. Overall, the proposed continuous-flow model demonstrates effective biowaste composting performance with potential heat generation, indicating its applicability for sustainable composting systems. Also, this model can assist in developing different biowaste treatment facilities in developing countries, contributing to long-term development goals.

Keywords: *Biowaste Composting, Continuous Composting, Forced Aeration, Biowaste Treatment, Numerical Modelling, Sustainability*

1. INTRODUCTION

Biowaste is the largest amount and most simply degradable component of municipal solid waste. It contains greenhouse gas emissions, odors, leachate pollution, and various human-health issues due to an inadequate management system. Aerobic and anaerobic composting are extensively recognized as sustainable bio-waste treatment processes due to stably composting organic matter, reprocessing nutrients, and reducing the overall amount of bio-waste (Ayilara et al., 2020; Saqib & Sadef, 2025). Over time, many composting methodologies have been discovered. These suggested from simple backyard piles and windrows to more advanced systems such as in-vessel reactors and aerated static piles (Azis et al., 2022; Manyapu et al., 2017; Onwosi et al., 2017). The main differences between these composting systems depend on air supply, process control, and handling high-moisture biowaste.

Windrows and static piles are simple and low-cost, but depend on maintaining oxygen and temperature, require large open areas, and often produce varying results (Onwosi et al., 2017; Saqib & Sadef, 2025). The aerated static pile systems suggest better control of air flow, temperature, and moisture. These composting systems produce compost more easily and consistently, although it require a large investment and functional costs. Different studies highlight that the selection of a composting method should consider performance, energy requirements, and suitability for proper urban settings where food and market waste control the organic waste (Manea et al., 2024).
Passive aeration depends on natural flow and diffusion of air through the compost mass and punctured pipes. Passively aeration of bio-waste composting, reducing the need for frequent waste mass removal while still achieving thermophilic conditions (Sołowiej et al., 2021). Although passive systems can stabilize biowaste and produce irregular temperature distributions compared to forced aeration (Bhave & Kulkarni, 2019; Kasinski et al., 2016; Veras et al., 2020). Comparisons show that while passive aeration is simple and cost-effective, forced aeration usually results in earlier stabilization and more uniform compost quality for bio-waste (Rasapoor et al., 2016). Forced aeration is one of the most important process improvements in bio-waste composting systems, either as positive aeration (air pushed upward/downward into the compost) or negative aeration (air pulled downward through suction), and sometimes using a combination of both(Finn A. Bondeson et al., 2023).

The encouragement of forced aeration on temperature distribution and degradation rates of biowaste has been studied through both experiments and mathematical modelling. Earlier studies by Bari et al. (2000) developed multilayer kinetic models for closed forced-aeration reactors and recognized that airflow rate strongly affects temperature patterns and biodegradation performance. Bari et al. (2012) extended this modelling approach to show how constant aeration shapes heat distribution and organic matter reduction. More recent modelling research has explored factors like aeration track, airflow, and re-circulation of air, highlighting the need for detailed models that connect aeration mode to heat, moisture, and degradation potential (Lai et al., 2024; Mihaela et al., 2021).
More development in composting methodology is the continuous or staged-continuous bio-waste composting systems, where fresh bio-waste is regularly added, and partially decomposed waste moves through other compartments. Reviews identify these systems as promising solutions for high-volume, steady biowaste generation in urban areas (Alves et al., 2023). Experimental work on multi-stage co-composting has shown that staged systems can achieve high degradation efficiency while finding better control of aeration and temperature in each phase (Alamin & Bari, 2022). Small-scale continuous reactors also show potential under both active and passive aeration, though temperature, moisture, and oxygen profiles can be highly variable.

Continuous composting and multi-slot reactors with layered compost beds and varying aeration rates are particularly relevant for treating wet municipal biowaste, whereas very few studies worked on bio-waste composting. So, potential mathematical models of continuous bio-waste composting can influence experimental studies on it. This Study focuses on biowaste composting in a continuous-flow reactor operated with upward forced aeration in a closed system by a mathematical model. The model develops and applies a numerical multilayer model that describes the spatio-temporal evolution of temperature, moisture content, biodegradable volatile solids, and oxygen demand in a multi-slot,

upward-aerated composting system, and evaluates its performance under realistic operating conditions. By integrating continuous material flow with forced aeration (both in terms of airflow magnitude and direction), the model aims to provide a quantitative framework for optimizing aeration strategies, retention time, and slot-wise operating conditions in biowaste composting systems based on upward forced aeration.

2. METHODOLOGY

2.1 Continuous-Flow Aerated Composting System

The numerical model of the continuous-flow aerated composting system works by successively moving bio-waste through seven aerated slots, confirming continuous biodegradation with upward forced aeration, as shown in Figure 1. Fresh bio-waste, denoted by key physicochemical components as temperature (T_c), specific heat transfer coefficient (K_c), composting mass (mc), moisture content (w), fixed solid (FS), non-volatile solids (NVS), biodegradable volatile solids (BVS), and reaction rate at temperature 25 °C (k_{25}), is placed into Slot 1. Each slot has six vertically layered (L1-L6), where air is supplied from the bottom and consistently distributed upward. The aeration pattern differs along the flow path: Slots 1-3 receive full airflow (Qi:12 m^3/h), Slots 4-6 operate at half airflow (Qi/2) to control heat from decomposition and support microbial activity during the shift from thermophilic to mesophilic conditions, and Slot 7 again receives Qi to provide final oxidation and moisture reduction. Bio-waste stays in each slot for 3 days, then the partially decomposed waste is moved to the next slot, while Slot 1 gets a new intake of incoming waste. This step-by-step process maintains a total retention time of 21 days, during which the aerated layers gradually transform the waste through active thermophilic breakdown, moisture evaporation, and stabilization. When the material reaches Slot 7, it is mature compost, indicated by decreased degradable carbon, decreased moisture, reduced volatile solids (VS) and total solids, and reduced oxygen demand. This continuous, layered, and serial flow design ensures effective aeration, even temperature distribution, and consistent compost quality throughout the system.

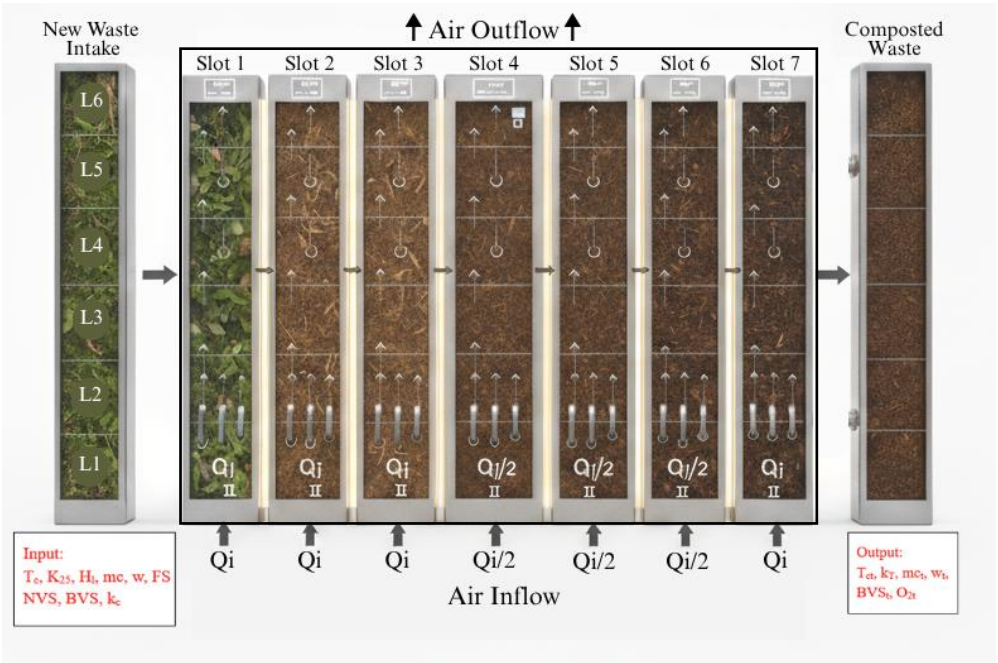

Figure 1: Proposed Material Flow Diagram of Continuous Composting

2.2 Model Description

Following earlier modelling methods for forced-aeration composting systems (Bari et al., 2000). The present model was developed based on the previous model to describe the spatiotemporal variation of temperature, moisture, degradable solids, and oxygen demand within a continuous-flow multi-slot composting reactor. In this configuration, the reactor consists of seven sequentially connected slots,

each containing six vertical layers through which air is supplied from the bottom and passed at the top. The basic mathematical formulation was derived considering heat and mass balance across each layer of the composting mass, following the generalized modelling principles used in previous kinetic and self-heating studies (Bari & Koenig, 2012), as shown in Equation 1. For each layer L_n (where n = 1, 2, …, 6), the model accounts for (i) heat accumulation in the compost matrix, (ii) heat inflow due to aeration, (iii) heat outflow through exhaust air, (iv) metabolic heat generation from biodegradation of biodegradable volatile solids (BVS), (v) sensible heat loss to the surroundings, and (vi) heat loss due to water evaporation and vapor transport. The airflow rate was explicitly incorporated into the formulation: Slots 1-3 receive full aeration (Qi), Slots 4-6 operate at half aeration (Qi/2), and Slot 7 receives Qi (Fig.1), reflecting the operational design of this continuous-flow system. The resulting layer-specific heat balance is expressed as Equation 1.

$$m_{c,t,L_n} \cdot C_{pc} \left(\frac{T_t - T_{t-1}}{dt}\right)_{L_n} = \dot{m}a_{i,L_{n-1}} \cdot C_{pa} \cdot T_{i,L_{n-1}} - \dot{m}a_{o,L_n} \cdot C_{pa} \cdot T_{t,L_n} + H_l - k_c \cdot C_{pc} \cdot m_{c,t,L_n}(T_{t,L_n} - T_a) - \frac{dw_{L_n}}{dt} \cdot L_e - \frac{dw_{v,L_{n-1}}}{dt} \cdot h_g + \frac{d(BVS_{L_n})}{dt} \quad (1)$$

Whereas, all the symbols of the equation are denoted in Table 1 as mc refers to the composting mass (waste mixture) in the reactor (kg), expressed as the sum of fixed solids (FS), non-biodegradable volatile solids (NVS), biodegradable volatile solids (BVS), and water (H_2O). The composting mass at any time t is denoted by mc_t. The total solids (TS) consist of FS and volatile solids (VS) in kg, with VS comprising both NVS and BVS. The degradation of BVS over time is represented by ΔBVS, expressed as a percentage. The water content of the composting mixture is indicated by w (as % of wet mass), while H_2O denotes the total water mass in the compost. Air inflow and outflow are described through $\dot{m}_{a_i}$(dry air mass inflow rate, kg.h^{-1}) and $\dot{m}_{a_o}$(dry air mass outflow rate, kg.h^{-1}), whereas Q_i indicates the airflow rate. The oxygen concentration in the composting mass at any time t is represented as O_{2t} (%).

Table 1. Definition of symbols used in the composting heat balance model

Symbol	Description (unit)	Symbol	Description (unit)
t	Time (h)	FS	Fixed solids (kg)
Δt	Time step for numerical integration (h)	VS	Volatile solids (kg)
L	Composting layer (–)	NVS	Non-biodegradable volatile solids (kg)
n	Layer number from bottom (–)	BVS	Biodegradable volatile solids (kg)
m_c	Initial composting mass in reactor (kg)	BVS_t	Biodegradable volatile solids at time t (kg)
m_{ct}	Composting mass at time t (kg)	w	Moisture content of compost (% wet basis)
T	Temperature (°C)	H_2O	Water content of compost (kg)
T_c	Initial compost temperature (°C)	w_{vi}	Water vapor in inlet air (kg/kg dry air)
T_{ct}	Compost temperature at time t (°C)	w_{vo}	Water vapor in outlet saturated air (kg/kg dry air)
T_t	Outlet air/compost temperature at time t (°C)	L_e	Latent heat of evaporation of water (kJ·kg^{-1})
T_a	Ambient air temperature (°C)	h_g	Enthalpy of saturated water vapor (kJ·kg^{-1})
$\dot{m}_i$	Dry air mass inflow rate (kg·h^{-1})	RH	Relative humidity of inlet air (%)
$\dot{m}_o$	Dry air mass outflow rate (kg·h^{-1})	O_{2t}	Oxygen concentration at time t (%)

Symbol	Description (unit)	Symbol	Description (unit)
Q_i	Airflow rate ($m^3 \cdot m^{-2} \cdot h^{-1}$)	f_w	Water production factor per unit BVS degraded ($kg \cdot kg^{-1}$)
C_{pc}	Specific heat capacity of wet compost ($kJ \cdot kg^{-1} \cdot °C^{-1}$)	f_{ea}	Gas production factor per unit BVS degraded ($kg \cdot kg^{-1}$)
C_{pa}	Specific heat capacity of dry air ($kJ \cdot kg^{-1} \cdot °C^{-1}$)	k_c	Heat transfer coefficient (h^{-1})
H_l	Heat released per unit BVS degradation ($kJ \cdot kg^{-1}$)	U	Overall heat transfer coefficient ($kJ \cdot h^{-1} \cdot m^{-2} \cdot °C^{-1}$)
k_T	Reaction rate constant at temperature T (h^{-1})	A	Heat transfer surface area (m^2)
k_{25}	Reaction rate constant at 25 °C (h^{-1})		

Water vapor terms include w_v(saturated water vapor mass per kg dry air), w_{vi}(water vapor in incoming air), and w_{vo}(saturated water vapor in outgoing air). The temperature of the composting mass is denoted by T, with T_c as the initial temperature and T_{ct} as the temperature at the time t. Ambient temperature is represented by T_a. The relative humidity (RH) influences moisture and vapor dynamics. Reaction rates are expressed through k_T(reaction rate at temperature T) and k_{25}(reaction rate at 25°C). The factors f_w, f_{ea}, and k_w account for water production per BVS degradation, gas formation per BVS degradation, and reaction rate reduction below 45% moisture, respectively. Thermal parameters include the specific heat capacity of wet composting material (c_{pc}) and dry air (c_{pa}). The heat generated due to BVS degradation is represented as H_l. Moisture evaporation and condensation processes are used h_g(enthalpy of saturated water vapor) and L_e(latent heat of evaporation). Heat transfer through reactor walls is governed by k_c, where $k_c = \frac{UA}{mc \cdot c_{pc}}$, with U representing the overall heat transfer coefficient and A the exposed surface area of the reactor. Finally, dt denotes the one-hour time interval used in the numerical model. Model performance was assessed using reference upward forced-aeration temperature data from a single six-layer composting unit, comparing measured and simulated temperatures.

2.3 Model Assumptions

The proposed model assumes a closed, continuous-flow composting reactor operated under upward forced aeration. The composting mass is divided into multiple slots and vertical layers, with variations in physico-chemical properties considered only in the vertical direction and horizontal gradients neglected. Initial waste properties are uniform for all simulations. Aeration rates are fixed within each slot according to the defined operating strategy. Each layer is represented by average temperature and moisture conditions. Biodegradable volatile solids degradation follows first-order kinetics dependent on temperature and moisture. Effects of pH variation, porosity changes, particle size distribution, and microbial population dynamics are neglected. The key model parameters and their adopted values are summarized in Table 2.

Table 2. Model Parameters and Initial Compost Composition Used in the Simulation

Model Parameters	Value	Unit	Initial Compost Composition	Initial Mass (kg)	Fraction (%)
Initial compost temperature	T_{ci}	27	°C	Total compost mass	118
Ambient air temperature	T_a	35	°C	Water	69.50
Heat generation per BVS	H_L	13,500	$kJ \cdot kg^{-1}$	Total solids (TS)	48.50

Model Parameters	Value	Unit	Initial Compost Composition	Initial Mass (kg)	Fraction (%)
Specific heat capacity of compost	c_{pc}	3.4	kJ·kg^{-1}·K^{-1}	Fixed solids (FS)	2.42
Heat transfer coefficient	k_c	5×10^{-5}	d^{-1}	Non-volatile solids (N-VS)	25.22
Reaction rate constant	k	0.00037	h^{-1}	Volatile solids (VS)	20.85
Relative humidity of the inlet air	RH_a	0.9	–	—	—
Inlet air vapor ratio	$Vapor_{in}$	0.0331	kg·kg^{-1}	—	—
Density of dry air	ρ_a	1.1399	kg·m^{-3}	—	—
Number of layers	–	6	–	—	—

3. RESULTS AND DISCUSSION

3.1 Temperature

The temperature growths at different points in the continuous-flow system of the model output are shown in Fig. 2(a-g). The temperature profile is presented slot-wise, reflecting the composting waste material progresses from one slot to the next while a fresh batch enters Slot 1 at each cycle. In Slot 1 (Fig. 2a), all six layers display a rapid temperature rise during the first three days of the first sample. The uppermost layer (L6) increased from 27 °C to about 50-52 °C, while L5 and L4 reached around 47 °C and 44 °C, respectively. The lower layers showed comparatively lower temperatures, with L1 rising to only about 33 °C due to absorbed direct air flow, indicating low microbial growth. This stratification is consistent with greater heat production and improved air movement in the upper region of the compost matrix due to higher microbial growth. The temperature difference in layers occurs due to oxygen supply, microbial growth, and heat retention varying across layers, causing upper layers to heat faster while lower layers lose heat more quickly for direct air absorption, as shown in Figure 3. In Fig. 2(b), where the first sample has transferred to Slot 2 and a new sample remains in Slot 1, the waste in Slot 2 exhibits a slightly moderated temperature profile. The peak temperatures in Slot 2 range between 33-48 °C for L1-L6, with a gradual decline thereafter, indicating reduced biological heat release as degradation progresses. The newly added material in Slot 1 again reaches similar peak values to those observed in Fig. 2(a), confirming the repeatability of the heating phase for each new intake. Same as in Figs. 2(c) and 2(d) show the temperature trends when the waste was passed to Slots 3 and 4. In Slot 3, the temperature peaks at approximately 46-48 °C for the upper layers and then begins a slight decline. The temperature increase is observed at the transition to Slot 4, where L6 reaches nearly 60-62 °C and L5 is close to 58-59 °C. This rise is attributed to the aeration pattern (airflow = Qi/2) and the availability of partially stabilized but still reactive organic matter.

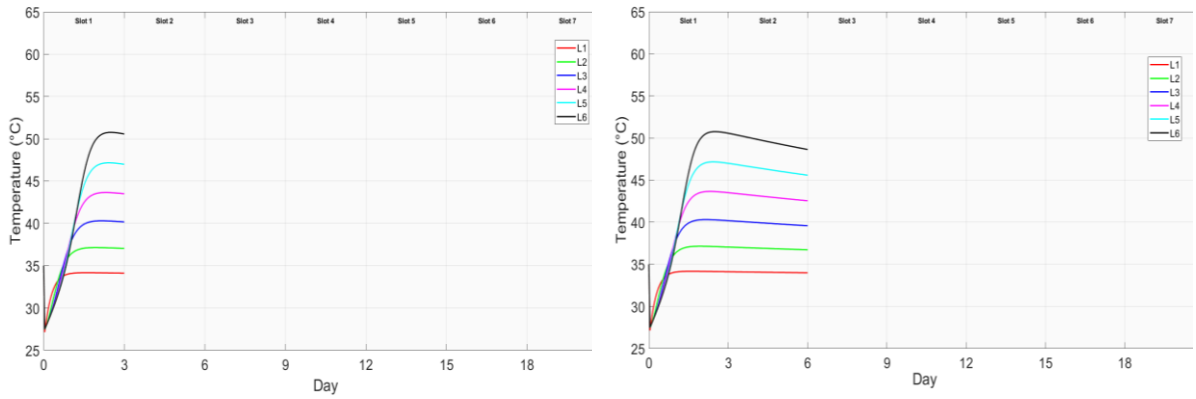

(a) (b)

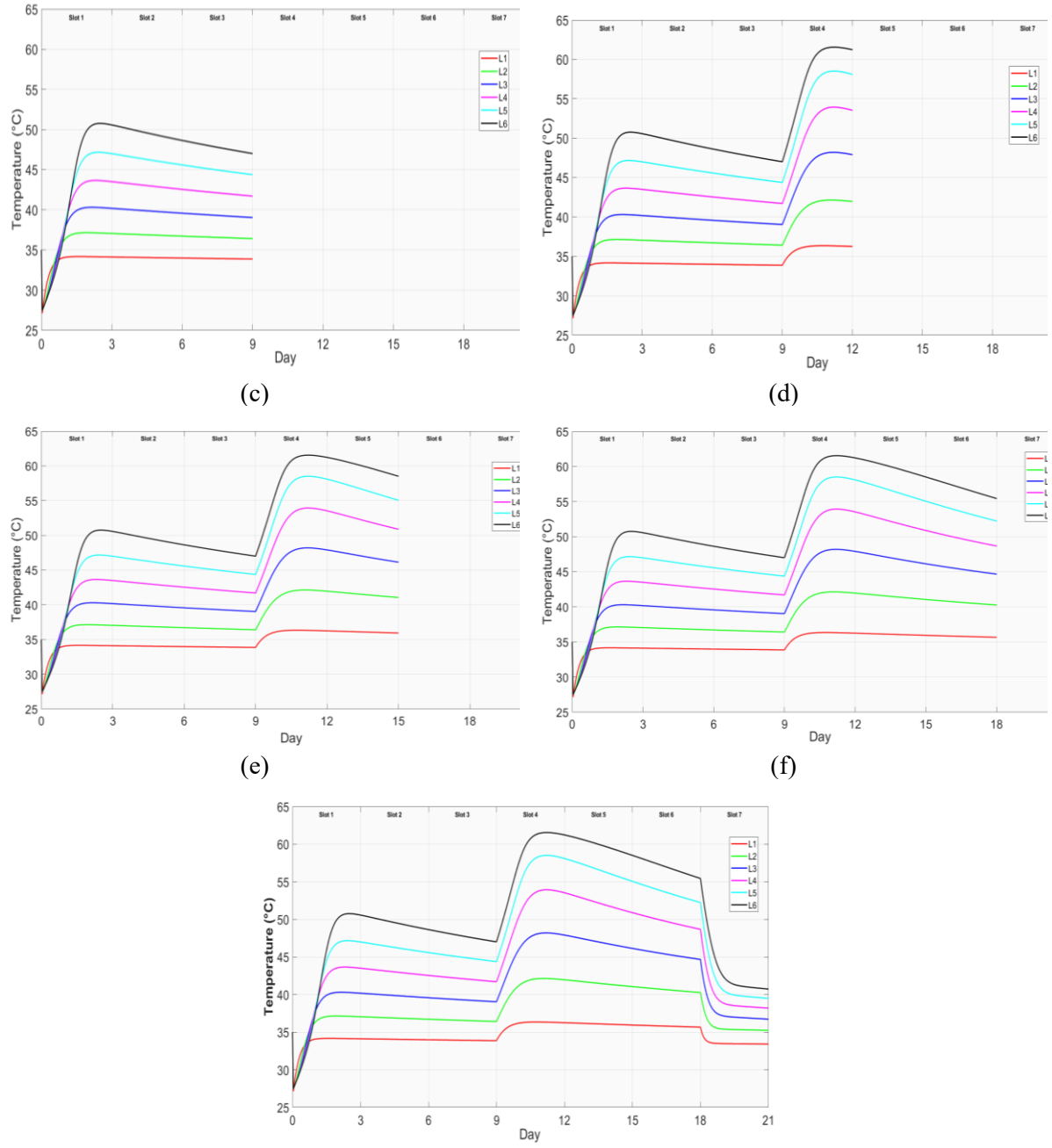

(c) (d)

(e) (f)

(g)

Figure 2: Temperature patterns for simulated composting with upward air flow; (a) slot 1, (b) slot 1-2, (c) slot 1-3, (d) slot 1-4, (e) slot 1-5, (f) slot 1-6, (g) slot 1-7

Figs. 2(e) and 2(f) illustrate the temperature behavior in Slots 5 and 6, where aeration is provided Qi/2. A gradual reduction in temperature occurs: L6 decreases from approximately 60 °C to about 50-52 °C ku during its residence in Slot 5, while Slot 6 temperatures further decline to around 45-48 °C. The lower layers (L1-L2) consistently remain in the 34-38 °C range, reflecting lower heating due to the decrease in the moisture of the waste sample. The complete seven-slot temperature development is presented in Fig. 2(g), whereas 7 samples are present in every slot. As waste reaches Slot 7, temperatures fall to around 40-43 °C in the upper layers and 32-35 °C in the lower layers, indicating the transition from the thermophilic to the cooling and maturation phase. The fresh sample in Slot 1 repeatedly shows the characteristic thermophilic rise, while the waste in Slot 7 exhibits the final stabilization stage. The observed temperature gradients across layers and slots confirm the expected thermophilic–mesophilic progression during continuous-flow operation and demonstrate that the imposed aeration pattern (Qi →

Qi/2 → Qi) maintained favorable thermal conditions throughout the composting cycle. Following the completion of a composting cycle, the continuous process of biowaste composting carries on progressively.

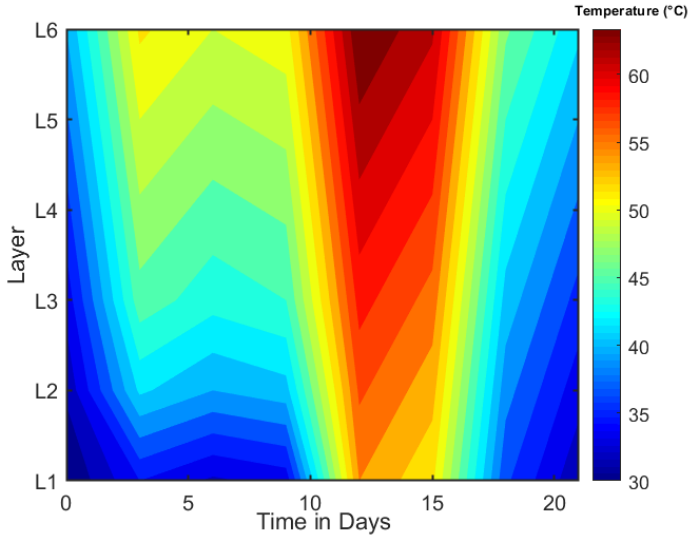

Figure 3: Temperature distribution over time and layer (Q 12 m^3/h)

3.2 Physico-chemical parameters

In this study, the simulation used an initial compost temperature of 27 °C and an ambient temperature of 35 °C. Key model parameters included HL = 13,500 kJ/kg, cpc = 3.4 kJ/kg·K, kc = 0.00005 d^{-1}, k = 0.00037 h^{-1}, RH_a = 0.8, vapor ratio = 0.02923, and air density = 1.1399 kg/m^3. The compost bed contained six layers with an initial mass of 118 kg, consisting of 69.5 kg water, 48.5 kg total solids, 2.42 kg free space, 25.22 kg non-volatile solids, and 20.85 kg volatile solids.

3.2.1 Volatile Solids (VS)

The decline in volatile solids across the six layers during the 21-day continuous-flow operation of the model is shown in Fig. 4(a). All layers showed a steady reduction in VS as the bio-waste proceeded from Slot 1 to Slot 7. VS decreased from an initial value of 21 kg to 14.7 (30%) kg in L1 and to 8.8 kg in L6 by Day 21 (58%). The upper layers (L5-L6) showed the highest rate of VS degradation, reflecting greater contact with aeration and elevated temperatures. In contrast, L1 and L2 exhibited a low degradation, consistent with concentrated oxygen availability and lower moisture retention in the lower compost layers.

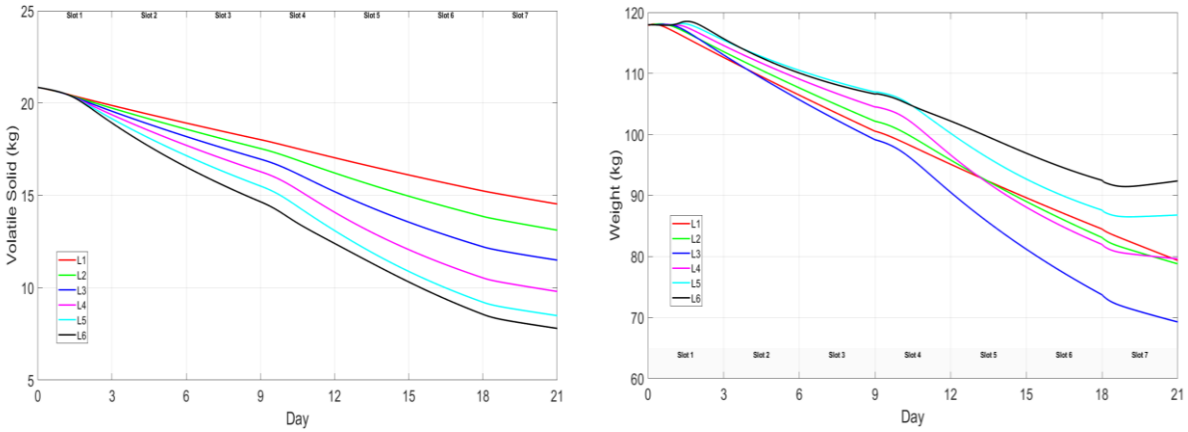

(a) (b)

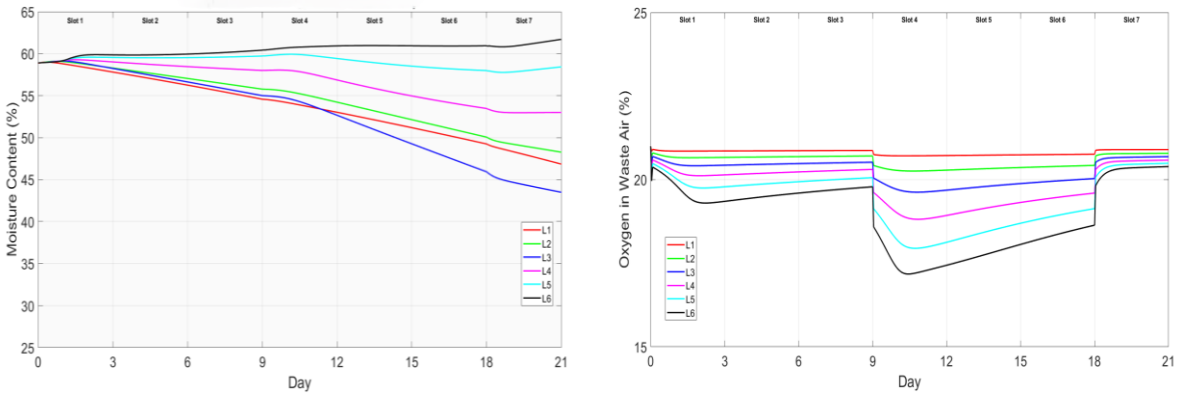

(c) (d)

Figure 4: Physico-chemical parameters pattern for simulated composting; (a) VS, (b) Waste composition, (c) Moisture Content, (d) Oxygen content in outflow air

3.2.2 Total Waste Weight

The overall total bio-waste mass loss pattern is illustrated in Fig. 4(b). The initial weight in all layers was input into the model as 118 kg, which declined progressively throughout the composting cycle. By Slot 7, L6 and L5 weights decreased to 86-92 kg of total waste, representing 22-27% reduction, whereas L3 maintained a higher final weight of about 69 kg, around a 52% reduction of total waste Because it maintains optimal temperature, moisture, and oxygen conditions, enabling maximum biodegradation and evaporation without excessive cooling or drying effects. The enhanced weight reduction in the upper layers corresponds to increased evaporation and faster organic degradation. A noticeable mass-loss acceleration appears during the change from Slot 3 to Slot 4, consistent with the elevated temperatures in that phase.

3.2.3 Moisture Content

Moisture content (%) trends for the six layers are presented in Fig. 4(c). Initial moisture content across layers (58%) changed as the compost moved through the slots. The upper layers (L5-L6) slightly increased their moisture level during the composting period due to upward vapor movement, and oxygen was accumulated for airflow, but subsequently declined at Slot 7. In the meantime, the lower layers (L1-L2) showed a more remarkable decrease, reaching about 45-48% by the end of the 21-day process. But in Layer 3 of the final slot, the moisture content decreased to 43% due to the middle layer of the compost pile. This gradual decline is associated with forced aeration, evaporative losses, and reduced metabolic water generation in the later stages.

3.2.4 Oxygen Concentration in Outflow Air

Fig. 4(d) shows the oxygen concentration in the used air for each layer as outflow of the model output. At the initial stage, oxygen levels ranged between 20-21% for the upper layers and lower layers. As the waste moved to Slots 2 and 3, oxygen consumption decreased first and then increased slightly, particularly in L4-L6, reflecting active microbial degradation. A substantial drop in oxygen concentration occurred in Slot 4 due to airflow to half (Qi/2), where L6 decreased to nearly 16-17%, corresponding to the thermophilic peak observed earlier, requiring careful aeration control to avoid anaerobic conditions. As biodegradation slowed in Slots 5 and 6, oxygen concentrations gradually increased. By the time the waste reached Slot 7, oxygen concentration recovered to around 20-21% in all layers for increased airflow to Qi.

3.3 Comparison of Experimental and Simulated

The experimental and simulated datasets were obtained from a previous study conducted by Bari & Koenig (2012). This study involved only one pile of waste composting, with six layers, whose pattern is similar to the continuous bio-waste composting model presented in the present study. In the previous

study, the waste had an initial moisture content of about 62.36% and a wet weight of 750 kg m^{-2}, with total solids (TS) of 37.64%. Fixed solids (FS) comprised about 4% of TS, while volatile solids (VS) accounted for 96.70%, equally divided between biodegradable (BVS) and non-biodegradable (NVS) fractions. The upward air flow was provided into the composting chamber average flow rate is 6.75 m3/hr. Fig 5. presents the comparison between experimental and simulated temperature profiles for six compost layers (L1-L6) under the upward forced-aeration composting system. The temperature evolution over a 21-day composting period is shown to illustrate the contrast between the measured behavior and the model-predicted thermal response of the multi-layer compost bed.

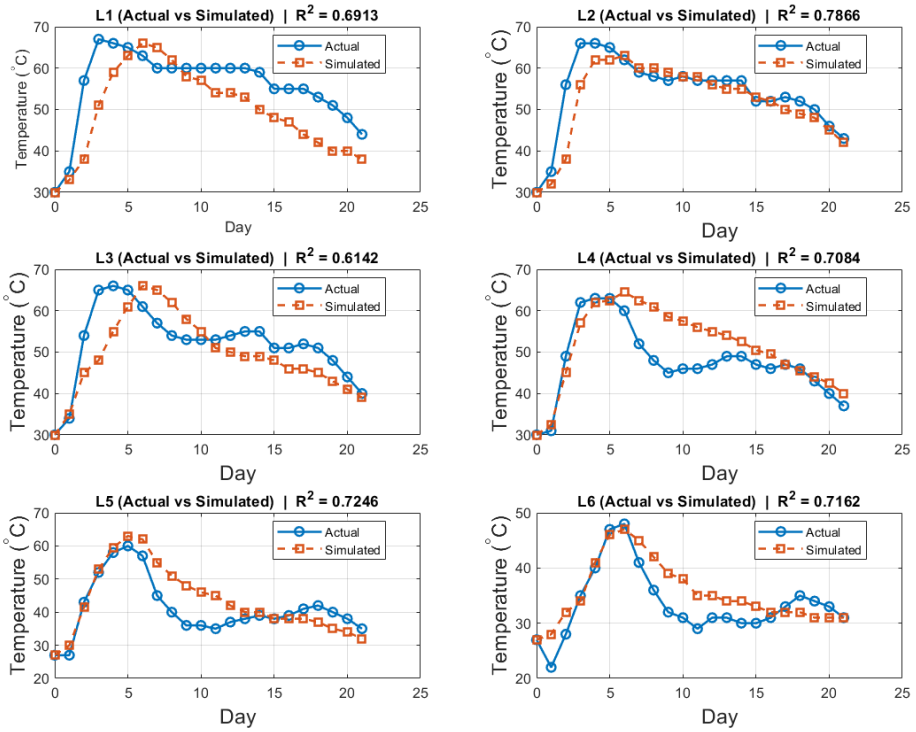

Figure 5: Comparison of Experimental and Simulated Temperature from the previous study

Across all layers, both the experimental and simulated profiles show the representative rapid temperature rise during the initial phase with the same air flow. Figure 5 shows that the proposed model reproduces the thermal evolution of the compost bed reasonably well for all six layers (L1–L6) under upward forced aeration. In each layer, the simulated profiles follow the main experimental trends, including the rapid temperature rise during the active thermophilic stage and the subsequent gradual cooling as biological activity declines. The model is supported by the coefficient of determination values (R^2 = 0.61–0.79) of L1-L6, indicating good predictive capability across the vertical compost depth. Overall, the model performance ensures that the proposed model performs well in capturing layer-wise temperature dynamics, and the observed performance indicates that continuous composting can be effective and suitable for real-time practical applications, supporting its applicability for further analysis and new model innovation of biowaste degradation and system performance. The comparison is limited by differences in waste composition, reactor geometry, and retention time; therefore, it serves only as qualitative validation rather than exact calibration of the model.

3.4 Engineering Significant

In developing countries, like Bangladesh, facing rapid urbanization, population growth, and the rising generation of biodegradable municipal waste. Major cities such as Dhaka, Chattogram, Khulna, Rajshahi, and Sylhet generate a large amount of biowaste every year, as shown in Table 3. Unmanaged and final disposed to open dumps, drains, non-sanitised landfills, or informal disposal sites, causing

greenhouse-gas emissions, leachate contamination, increasing odour, and significant public-health risks. Establishing large-scale continuous biowaste composting plants, as modeled in this study, with suggested forced aeration offers a significantly robust and sustainable solution to this challenge. Furthermore, continuous-composting flow systems ensure nonstop biowaste treatment, stable thermophilic conditions, and consistent conversion of organic waste into nutrient-rich compost, while minimizing land requirements and operational variability. The model demonstrated in this study provides a strong engineering basis for designing high-efficiency composting reactors with optimized aeration, layer-wise heat distribution, and reliable degradation performance suitable for high-moisture urban biowaste. Also, the model outcomes guide reactor design by defining optimal reactor height, number of layers, residence time, and airflow distribution required to maintain thermophilic conditions and efficient biodegradation. Implementing this technology in Bangladesh would contribute directly to national goals for sustainable waste management, climate-change mitigation, soil fertility improvement, and advancement of a circular bioeconomy. Thus, continuous large-scale composting plants represent a transformative engineering intervention for ensuring sustainable growth in Bangladesh's major metropolitan regions.

Table 3: Biowaste Generation in Major Cities of Bangladesh

City	Bio-waste generation (ton/year)	Reference
Dhaka	1,364,000	(Abedin & Jahiruddin, 2015; Ahmed et al., 2023)
Chattogram	336,000	
Khulna	133,000	
Rajshahi	43,000	
Barishal	33,000	
Sylhet	55,000	

4. CONCLUSIONS

This study develops a numerical model to explain continuous-flow biowaste composting under upward forced aeration, addressing a key limitation in current models that mainly emphasize closed systems. The multi-layer, multi-slot approach links thermal behaviour, biodegradation, and air-moisture transport, and accurately reflects patterns commonly observed in real composting operations. The simulation shows that the designed aeration sequence (Qi=12 kg/m^3 in early slots, Qi/2 in mid-slots, and Qi in the final stage) effectively supports the required thermophilic-to-mesophilic transition for pathogen reduction, rapid decomposition, and moisture regulation. Temperature, volatile-solids degradation (30-58%), and oxygen-consumption profiles demonstrate the importance of layer-specific aeration and moisture distribution in determining overall system performance. The stepwise movement of material through seven slots ensures consistent thermophilic conditions during early processing and adequate cooling and stabilization in later stages. Model predictions closely matched background experimental data (temperature), with the simulated R^2: 0.61–0.79, confirming its reliability for evaluating system performance. Overall, the findings offer useful guidance for optimizing aeration rates, residence time, and layer design in engineered composting systems, particularly for high-moisture urban biowaste. Future enhancements may include modelling gas emissions, dynamic aeration control, and detailed moisture redistribution to further improve predictive accuracy.

AI Declaration

The author declares that AI-based tools were used solely for language improvement and grammatical correction during the preparation of this manuscript.

REFERENCES

Abedin, M. A., & Jahiruddin, M. (2015). Asian Journal of Medical and Biological Research Waste generation and management in Bangladesh: An overview. *Asian J. Med. Biol. Res*, *2015*(1), 114–120. www.ebupress.com/journal/ajmbr

Ahmed, Md. J., Taher, M. A., & Reza, Md. A. A. (2023). Solid Waste Generation, Composition and Potentiality of Waste-to-Resource Recovery in Sylhet City Corporation, Bangladesh. *Green Building & Construction Economics*, 306–322. https://doi.org/10.37256/gbce.4220232657

Alamin, Md., & Bari, Q. H. (2022). Extent of degradation in three stage co-composting of fecal sludge and solid waste. *Journal of the Air & Waste Management Association*, *72*(8), 914–924. https://doi.org/10.1080/10962247.2022.2064936

Alves, D., Villar, I., & Mato, S. (2023). Community composting strategies for biowaste treatment: methodology, bulking agent and compost quality. *Environmental Science and Pollution Research*, *31*(7), 9873–9885. https://doi.org/10.1007/s11356-023-25564-x

Ayilara, M., Olanrewaju, O., Babalola, O., & Odeyemi, O. (2020). Waste Management through Composting: Challenges and Potentials. *Sustainability*, *12*(11), 4456. https://doi.org/10.3390/su12114456

Azis, F. A., Rijal, M., Suhaimi, H., & Abas, P. E. (2022). Patent Landscape of Composting Technology: A Review. *Inventions*, *7*(2), 38. https://doi.org/10.3390/inventions7020038

Bari, Q. H., & Koenig, A. (2012). Application of a simplified mathematical model to estimate the effect of forced aeration on composting in a closed system. *Waste Management*, *32*(11), 2037–2045. https://doi.org/10.1016/j.wasman.2012.01.014

Bari, Q. H., Koenig, A., & Guihe, T. (2000). Kinetic analysis of forced aeration composting - I. Reaction rates and temperature. *Waste Management*, 303–312.

Bhave, P. P., & Kulkarni, B. N. (2019). Effect of active and passive aeration on composting of household biodegradable wastes: a decentralized approach. *International Journal of Recycling of Organic Waste in Agriculture*, *8*(S1), 335–344. https://doi.org/10.1007/s40093-019-00306-7

Finn A. Bondeson, Joshua W. Faulkner, & Eric D. Roy. (2023). *Performance of a Compost Aeration and Heat Recovery System at a Commercial Composting Facility*.

Kasinski, S., Slota, M., Markowski, M., & Kaminska, A. (2016). Municipal waste stabilization in a reactor with an integrated active and passive aeration system. *Waste Management*, *50*, 31–38. https://doi.org/10.1016/j.wasman.2016.02.012

Lai, J. C., Then, Y. L., Hwang, S. S., & Lee, C. S. (2024). Optimal aeration management strategy for a small-scale food waste composting. *Carbon Resources Conversion*, *7*(1), 100190. https://doi.org/10.1016/j.crcon.2023.06.002

Manea, E. E., Bumbac, C., Dinu, L. R., Bumbac, M., & Nicolescu, C. M. (2024). Composting as a Sustainable Solution for Organic Solid Waste Management: Current Practices and Potential Improvements. *Sustainability*, *16*(15), 6329. https://doi.org/10.3390/su16156329

Manyapu, V., Shukla, S., Kumar, S., & Rajendra, K. (2017). *In-Vessel Composting: A Rapid Technology for Conversion of Biowaste into Compost*. *www.oaijse.com*

Mihaela Marian, N., digitale del, F., candidato, della, & Cecilia Viti, T. (2021). *The Role of Mineralogy in Circular Economy: From Inorganic Special Wastes to Secondary Raw Materials Firmato.*

Onwosi, C. O., Igbokwe, V. C., Odimba, J. N., Eke, I. E., Nwankwoala, M. O., Iroh, I. N., & Ezeogu, L. I. (2017). Composting technology in waste stabilization: On the methods, challenges and future prospects. *Journal of Environmental Management*, *190*, 140–157. https://doi.org/10.1016/j.jenvman.2016.12.051

Rasapoor, M., Adl, M., & Pourazizi, B. (2016). Comparative evaluation of aeration methods for municipal solid waste composting from the perspective of resource management: A practical case study in Tehran, Iran. *Journal of Environmental Management*, *184*, 528–534. https://doi.org/10.1016/j.jenvman.2016.10.029

Saqib, Z., & Sadef, Y. (2025). Sustainable waste management through commercial composting: Challenges, opportunities, and future directions for circular economy. *European Journal of Sustainable Development Research*, *9*(4), em0319. https://doi.org/10.29333/ejosdr/16579

Sołowiej, P., Pochwatka, P., Wawrzyniak, A., Łapiński, K., Lewicki, A., & Dach, J. (2021). The Effect of Heat Removal during Thermophilic Phase on Energetic Aspects of Biowaste Composting Process. *Energies*, *14*(4), 1183. https://doi.org/10.3390/en14041183

Veras, R. S., Stefanutti, R., Lima, A. C. A. de, & Magalhães, G. (2020). Compostagem de resíduos urbanos em leiras estáticas com aeração passiva. *Revista DAE*, *68*(224), 166–181. https://doi.org/10.36659/dae.2020.047